Journal of Thermal Analysis and Calorimetry (2019) 138:163–173
https://doi.org/10.1007/s10973-019-08211-x

The synthesis, characterization and effect of molar mass distribution on solid-state degradation kinetics of oligo(orcinol)

Fatih Doğan[1,2] · Naciye Özdek[3] · Nursel Acar Selçuki[3] · İsmet Kaya[1]

Received: 8 September 2018 / Accepted: 22 March 2019 / Published online: 30 March 2019

Abstract
In this study, the oxidative polymerization of orcinol monohydrate using different oxidants such as NaOCl, H_2O_2, and air was investigated. Polymerization studies were carried out between 50 and 90 °C. The optimum reaction conditions of the polymerization were also established. NaOCl was found to be the most active oxidant. The characterization of oligo(orcinol) was conducted by using FT-IR, ^{1}H-NMR and ^{13}C-NMR, TGA, size exclusion chromatography (SEC) and solubility techniques. At the optimum reaction conditions, the conversion to oligomer of orcinol was found to be 62% (for NaOCl oxidant), 42% (for H_2O_2 oxidant), and 21% (for air oxidant). According to the SEC analysis, the number-average molecular mass (M_n), mass-average molecular mass (M_w) and polydispersity index (PDI) values of oligo(orcinol) were determined to be 2260, 2540 g mol^{-1}, and 1.12, using NaOCl, and 2170, 2470 g mol^{-1}, and 1.14, using H_2O_2 and 1500, 1770 g mol^{-1}, and 1.18, using air, respectively. In addition, the relationship between molar mass distributions and activation energies of thermal degradation processes of oligo(orcinol) was investigated by using TG analysis. For this purpose, the methods based on multiple heating rates such as Flynn–Wall–Ozawa [FWO], Tang, and Kissinger–Akahira–Sunose [KAS] were used. The activation energy related to the solid-state decomposition of oligo(orcinol) synthesized with NaOCl oxidant was calculated to be 79.02 kJ mol^{-1} by KAS method, 78.74 kJ mol^{-1} by Tang method and 81.78 kJ mol^{-1} by FWO method in the range of $0.05 < \alpha < 0.95$. The results obtained show that activation energy increased with an increase in molar mass.

Keywords Oxidative polymerization · Thermal analysis · Non-isothermal thermal degradation kinetics

Introduction

The NaOCl used for oxidative polycondensation of phenols having low activity is believed to be the most active oxidizing agent [1, 2]. There are advantages of H_2O_2 oxidant as it transforms to water without forming any byproduct. On the other hand, H_2O_2 provides that the phenols react to yield oxidative polycondensation at low temperatures (20–50 °C) in the presence of little amount of some catalysts (1–2%). H_2O_2 is much more expensive compared to the other oxidants. The air oxygen is the most suitable oxidant for oxidative polycondensation reaction since it is very cheap and abundant. Moreover, it forms only water during the reaction as byproduct, which is the most important advantage of oxygen. However, since the air oxygen is a mild oxidant, it is not utilizable for polymerization of the phenols. Oxidative polymerization of phenol is carried out without catalyst in polar solvents such as water, tetrahydrofuran, alcohol, acetic acid. From this point of view, the most important solvent is water because it is cheap and safe and removed readily. On the other hand, there are two kind of coupling in oxidative polymerization of phenol derivatives. These are C–C and C–O–C couplings. These couplings can take place during polymerization. Kobayashi and Higashimura have studied on

✉ İsmet Kaya
kayaismet@hotmail.com; ikaya@comu.edu.tr

[1] Polymer Synthesis and Analysis Lab, Department of Chemistry, Faculty of Science and Arts, Canakkale Onsekiz Mart University, 17020 Canakkale, Turkey

[2] Secondary Science and Mathematics Education, Faculty of Education, Canakkale Onsekiz Mart University, 17010 Canakkale, Turkey

[3] Department of Chemistry, Faculty of Science, Ege University, 35100 Izmir, Turkey

coupling selectivity [3]. The reaction mechanisms of the selectivity for C–O coupling, however, have not been made thoroughly clear yet. First, the following three reaction mechanisms so far proposed are discussed: (1) coupling of the free phenoxy radicals, (2) coupling of the phenoxy radicals coordinated to catalyst complexes, and (3) coupling through the phenoxonium cation. Next, an oxidoreductase enzyme such as peroxidase or oxidase and a peroxidase model complex that have been recently found as the catalyst for oxidative polymerization of phenols are described. In 1959, Hay and co-workers discovered an oxidative polymerization of 2,6-Me_2P catalyzed by CuCl/pyridine (Py) under dioxygen leading to poly(2,6-dimethyl-1,4- phenylene oxide) (P-2,6-Me_2P) [4]. This is the first example for oxidative polymerization to synthesize a phenolic polymer with high molecular mass. This kind of phenol derivatives has some useful properties like paramagnetism, semi-conductivity, stability in the effect of high energy. Because of these properties, they are used in preparing composites that have done high stability at high temperature, thermostabilizer, graphite materials, epoxy oligomer and block copolymer, photoresist and in preparing antistatic and flame resistant materials. These polymers can gain new and useful properties adding different functional groups in their structure. Until today, effects of these additional functional groups on the main chain have been reported by several works [5–11]. In addition, polyphenols that have various functional groups can be used for cleaning process of toxic heavy metals in industrial wastewater. For this reason, the synthesis of polymer-metal complex is very important for analytic and environmental chemistry. Considering these advantages, polymer structured ligands have been prepared and complex forms have been tried with many of transition metals. Thus, polyphenols have a wide usage area.

In this study, oxidative polymerization of orcinol monohydrate was firstly carried out in aqueous alkaline solution by using different oxidants such as NaOCl, H_2O_2, and air. The dependence of monomer conversion on various reaction parameters, including reaction time, temperature, as well as the amount of oxidant was also investigated. The structure of the oligo(orcinol) was confirmed by FT-IR, ^{1}H-NMR, ^{13}C-NMR and TG techniques. Then, molar mass distributions of oligo(orcinol) were determined by SEC analysis. The determination of relationship between activation energy and molar mass distributions of oligo(orcinol) was purposed. Finally, activation energy related to the solid-state thermal degradation of oligo(orcinol)s was separately determined by using methods based on multiple heating rate.

Materials and methods

Materials

Orcinol monohydrate was supplied from Fluka. Hydrogen peroxide (30%, H_2O_2), potassium hydroxide (KOH) and all solvent were supplied from Merck, and used without further purification. Sodium hypochlorite (30% aqueous solution) was supplied from Paksoy chemical company.

Polymerization of orcinol monohydrate

The orcinol monohydrate was polymerized in alkaline medium with different oxidants such as NaOCl, H_2O_2 and air. The polymerization was carried out by the following procedures: first of all (0.0144 g, 1×10^{-3} mol) orcinol monohydrate was dissolved in 0.1 M KOH solution (1×10^{-3} mol) and the final solution was introduced to a three-necked glass. Flask was stirred with a magnetic stirrer and fitted with a thermometer, a dropping funnel which contains either NaOCl (30%) or H_2O_2 solution and a condenser. After heating at 40 °C for 30 min, H_2O_2 was added dropwise over about 20 min. The mixture was heated at various temperatures and times. In case of using air as oxidant, the air was passed in at rate of 8.5 L h^{-1} during the course of the reaction. In order not to have water loss in the reaction mixture and to neutralize the CO_2 of air to KOH, air was passed into 200 mL of an aqueous solution of KOH (20%) before sending into the reaction tube. The mixture was heated at various temperatures and times. In the end of all the polymerization methods, it was cooled to room temperature and then 3 mL of HCl (37%) was added to the reaction mixture. The mixture was filtered, washed with hot water (50 mL × 3), for separating from mineral salts and unreacted monomer, and then dried in the vacuum oven at 50 °C. The general procedure is described in Scheme 1.

Characterization techniques

The infrared spectra were obtained on PerkinElmer Spectrum One FT-IR system using universal ATR sampling accessory within the wavelengths of 4000–650 cm^{-1}. ^{1}H-NMR and ^{13}C-NMR spectra (Bruker Avance DPX-400 and

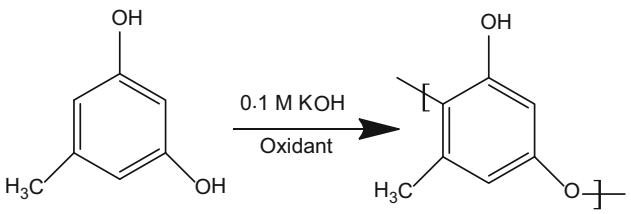

Scheme 1 Synthetic rough for oligo(orcinol)

100.6 MHz, respectively) were recorded at room temperature in deuterated DMSO. TMS was used as internal standard. SEC analyses were performed at 30 °C using DMF/MeOH (v/v, 4/1) as eluent at a flow rate of 0.4 mL min^{-1}. The instrument (Shimadzu 10AVp series HPLC-SEC system) was calibrated with a mixture of polystyrene standards (Polymer Laboratories; the peak molecular masses, M_p, between 162 and 19880) using GPC software for the determination of the molecular mass (M_n), mass-average molecular mass (M_w) and polydispersity index (PDI) of the polymer sample. Macherey–Nagel GmbH & Co. (100 Å and 7.7 nm diameter loading material) 3.3 mm i.d. × 300 mm columns were used for SEC analyses. The TG measurements were taken using a PerkinElmer Diamond Thermal Analysis in dynamic nitrogen atmosphere at a flow rate of 200 mL min^{-1} up to 1273 K. The heating rates were 5, 10, 15 and 20 °C min^{-1} and sample sizes ranged in mass from 8 to 10 mg. A platinum crucible was used as sample container.

Kinetic study

In studying the thermal degradation kinetics, model-free methods reported in the literature were chosen: Tang method [12], Kissinger–Akahira–Sunose method (KAS) [13–16] and Flynn–Wall–Ozawa method (FWO) [17–19] that can be expressed by following equations.

Model-free methods

Tang method

Tang method can be expressed by Eq. (1)

$$\ln\left(\frac{\beta}{T^{1.894661}}\right) = \ln\left(\frac{AE}{Rg(a)}\right) + 3.635041 - 1.894661\ln E - \frac{1.001450E}{RT} \quad (1)$$

In here, α, $g(\alpha)$, T, R, E, A are degradation fraction, integral function of degradation, absolute temperature, pre-exponential factor and gas constant, respectively. Activation energy can be obtained from the slope of Arrhenius lines calculated for the same degradation values at different heating rates.

Kissinger–Akahira–Sunose method

Kissinger–Akahira–Sunose (KAS) method is an isoconversional method like Tang method. Equation (2) suggested by KAS was also utilized to determine the values of activation energy from plots of $\ln(\beta/T^2)$ against $1/T$ over a wide range of conversion.

$$\ln\left[\frac{\beta}{T^2}\right] = \ln\left[\frac{AR}{Eg(a)}\right] - \frac{E}{RT} \quad (2)$$

The slope of line drawn between $\ln(\beta/T^2)$ versus $1/T$ gives activation energy.

Flynn–Wall–Ozawa method

The Flynn–Wall–Ozawa method is an integral method, and the so-called Eq. (3) suggested by FWO can be used in logarithmic form for determining the activation energy of a solid-state thermodegradation process. Pre-exponential factor, A, and activation energy, E, are not depend on degradation fraction, but they depend on the temperature. This method uses Eq. (3)

$$\log g(\alpha) = \log\frac{AE}{R} - \log\beta + \log p\left(\frac{E}{RT}\right) \quad (3)$$

If $E/RT \geq 20$, Doyle approximation is used and Eq. (4) can be obtained

$$\log\beta = \log\frac{AE}{R} - \log g(\alpha) - 2.315 - 0.4567\frac{E}{RT} \quad (4)$$

The slope of line drawn between $\log(\beta)$ versus $1/T$ gives activation energy.

Results and discussion

Oxidative polycondensation of orcinol with different oxidants

The optimum conditions of oxidative polycondensation reactions of orcinol with different molar mass distributions were determined. Orcinol was polymerized in aqueous alkaline solution via phenoxy radicals using NaOCl, H_2O_2 and air as oxidant at various conditions such as temperature, reaction time and concentration of the initiator. It was observed that the conversion to oligomer varied depending on the conditions and type of the oxidants.

Oxidative polycondensation of orcinol in presence of NaOCl as oxidant

The optimum reaction conditions of orcinol were investigated in an aqueous alkaline medium by using NaOCl as oxidant [20]. When orcinol monomer interacted with these oxidants in an aqueous alkaline medium, brown phenoxy radicals immediately precipitated in the solution medium. The experiments were carried out over a range of temperature 40–90 °C with NaOCl as an oxidant depending on

time. It was observed that the yield increased up to 70 °C while it decreased at 90 °C. The reason of this is the degradation of the polymer back to monomer [21]. The reaction was run as long as 3–24 h. The optimum reaction time was found to be 10 h. The conversion decreased with the decreasing KOH concentration. The highest conversion at suitable conditions was found to be 62%. The % conversion values under different reaction conditions are given in Table 1. Briefly, the conversion of orcinol was 62% at conditions such as $[orcinol]_0 = 0.0144$ mol L^{-1}, $[KOH]_0 = 0.024$ mol L^{-1} and $[NaOCl]_0 = 0.04$ mol L^{-1}, at 70 °C for 10 h. It is seen that in Table 1, the conversion of oligomer generally increased in increasing of reaction temperature. But the conversion of oligomer decreased in increasing of reaction times at the same reaction temperatures. At the same conditions, when initial molar amount of KOH was decreased, the conversion to oligomer of orcinol was changed from 53 to 62%.

Oxidative polycondensation of orcinol in presence of H_2O_2 as oxidant

The oxidative polycondensation of orcinol was carried out using H_2O_2 (30%) as oxidant. The highest conversion to oligomer was obtained at 70 °C. It was also seen that the conversion to oligomer was decreased above 70 °C due to the thermal degradation. The experiments were run for 3–20 h in order to determine the effect of reaction time on the % conversion. The highest conversion to oligomer which is 42% was obtained in the experiment run for 15 h. The conversion to oligomer of orcinol decreased with the increasing H_2O_2 concentration. The % conversion values under different reaction conditions are given in Table 2. At the same conditions, when the molar amount of alkaline was increased in approximately two coatings, the total conversion to oligomer orcinol was changed from 26 to 30%. According to these values, H_2O_2 is not a very good oxidant for orcinol. The conversion to oligomer of orcinol was 42% at optimum conditions such as $[orcinol]_0 = 0.0144$ mol L^{-1}, $[KOH]_0 = 0.0430$ mol L^{-1} and $[H_2O_2]_0 = 0.03$ mol L^{-1}, at 70 °C for 15 h.

Oxidative polycondensation of orcinol with air

The experiments were run over a range of temperature 50–80 °C by using air. It was observed that the conversion to oligomer was increased up to 50 °C while it was decreased above 50 °C. The reason is the degradation of the oligomer back to monomer. The reaction time was chosen as 3–20 h in different times. The optimum reaction time was found to be 3 h. The highest conversion was found to be 21%. The conversion to oligomer values under different conditions is given in Table 3.

By using air as the oxidant, the conversion to oligomer of orcinol was 21% at optimum conditions such as $[orcinol]_0 = 0.0144$ mol L^{-1} and $[KOH]_0 = 0.0430$ mol L^{-1} at

Table 1 The oxidative polycondensation reaction parameters of oligo(orcinol) with NaOCl in aqueous KOH

Run	Temperature/°C	Time/h	$[KOH]_0$/mol L^{-1}	$[NaOCl]_0$/mol L^{-1}	Conversation of orcinol/%
1	40	3	0.043	0.03	08
2	50	3	0.043	0.03	11
3	60	3	0.043	0.03	15
4	70	3	0.043	0.03	22
5	80	3	0.043	0.03	20
6	90	3	0.043	0.03	18
7	70	5	0.043	0.03	25
8	70	10	0.043	0.03	49
9	70	15	0.043	0.03	45
10	70	20	0.043	0.03	42
11	70	24	0.043	0.03	40
12	70	10	0.043	0.04	53
13	70	10	0.043	0.05	51
14	70	10	0.043	0.09	48
15	70	10	0.043	0.12	46
16	70	10	0.024	0.04	62
17	70	10	0.012	0.04	58
18	60	10	0.006	0.04	44
19	60	10	0.003	0.04	38

Monomer concentration was used as 0.0144 mol L^{-1} in reactions

Table 2 The oxidative polycondensation reaction parameters of oligo(orcinol) with H_2O_2 oxidant in aqueous KOH

Run	Temperature/°C	Time/h	$[KOH]_0$/mol L^{-1}	$[H_2O_2]_0$/mol L^{-1}	Conversation of orcinol/%
1	50	3	0.043	0.03	11
2	60	3	0.043	0.03	14
3	70	3	0.043	0.03	17
4	80	3	0.043	0.03	13
5	70	5	0.043	0.03	26
6	70	10	0.043	0.03	34
7	70	15	0.043	0.03	42
8	70	20	0.043	0.03	37
9	70	10	0.043	0.01	28
10	70	10	0.043	0.06	30
11	70	10	0.032	0.03	26
12	70	10	0.024	0.03	18

Monomer concentration was used as 0.0144 mol L^{-1} in reactions

Table 3 The oxidative polycondensation reaction parameters of oligo(orcinol) with air in aqueous KOH

Run	Temperature/°C	Time/h	[KOH]/mol L^{-1}	Air/L h^{-1}	Conversation of orcinol/%
1	50	3	0.043	8.5	21
2	60	3	0.043	8.5	16
3	70	3	0.043	8.5	12
4	80	3	0.043	8.5	10
5	50	5	0.043	8.5	14
6	50	10	0.043	8.5	9
7	50	15	0.043	8.5	12
8	50	20	0.043	8.5	11

Monomer concentration was used as 0.0144 mol L^{-1} in reactions

Table 4 Solubility of orcinol and oligo(orcinol)

Compounds	NMP	DMSO	DMF	H_2SO_4	THF	Toluene	CCl_4	Hexane	Heptane
Orcinol	+	+	+	+	+	−	−	−	−
Oligo(orcinol)	+	+	+	+	±	−	−	−	−

+, soluble at room temperature; ±, partly soluble at room temperature; −, soluble at room temperature

Table 5 Molar mass distribution of oligo(orcinol)

Compound	Total			Fraction-I				Fraction-II				Fraction-III			
	M_n	M_w	PDI	M_n	M_w	PDI	%	M_n	M_w	PDI	%	M_n	M_w	PDI	%
Oligo(orcinol)[a]	2260	2540	1.12	3400	3800	1.12	60	9900	11,400	1.15	35	25,600	26,750	1.15	5
Oligo(orcinol)[b]	2170	2470	1.14	2000	2850	1.43	61	8000	8200	1.03	39	–	–	–	
Oligo(orcinol)[c]	1500	1770	1.18	1800	2400	1.33	79	7600	7800	1.03	21	–	–	–	

[a]The oligomer which is synthesized by NaOCl as oxidant

[b]The oligomer which is synthesized by H_2O_2 as oxidant

[c]The oligomer which is synthesized by air as oxidant

50 °C for 3 h. As seen from Tables 1, 2 and 3, in these reactions, the conversion to oligomer was dependent upon temperature, times and initial concentrations of alkaline and oxidants. At the same conditions, the conversion to oligomer of orcinol with H_2O_2 and air was less than NaOCl [22]. The all characterization procedures were performed using the products obtained from the higher conversion for each oxidant

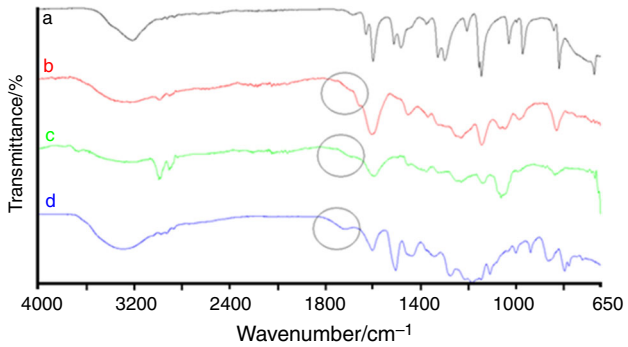

Fig. 1 FT-IR Spectra of orcinol (**a**) and oligo(orcinol) synthesized by NaOCl (**b**), H_2O_2 (**c**), air (**d**) oxidants

Solubility and structure analysis of oligo(orcinol)

The solubility tests were carried out in different solvents by using 1 mg sample and 1 mL solvent at 25 °C. The synthesized oligo(orcinol) derivatives have dark color powder form and have higher solubility in polar solvents such as DMSO, DMF and concd. H_2SO_4. Yet, they are insoluble in aprotic solvents such as toluene, CCl_4, hexane, and heptane (Table 4). SEC analysis of oligo(orcinol) was carried out using DMF/methanol (4/1) as eluent at 25 °C, with a flow rate of 0.4 mL min^{-1}.

It was observed in SEC analysis of the oligo(orcinol) that the one obtained according to molar mass in presence of NaOCl formed three fractions as those obtained with air oxygen and with H_2O_2 formed two fractions (Table 5). For oligo(orcinol) synthesized by NaOCl as oxidant, low molar mass fraction was formed 35% (M_n: 9900 g mol^{-1}, M_w: 11,400 g mol^{-1}, PDI: 1.15) and 60% (M_n: 3400 g mol^{-1}, M_w: 3800 g mol^{-1}, PDI: 1.12) and high molar mass fraction was formed 5% (M_n: 25,600 g mol^{-1}, M_w: 26,750 g mol^{-1}, PDI: 1.15). For oligo(orcinol) synthesized by H_2O_2 as oxidant, low molar mass fraction formed 61% of the oligomer (M_n: 2000 g mol^{-1}, M_w: 2850 g mol^{-1}, PDI: 1.43)) while higher one is found in proportion 39% (M_n: 8000 g mol^{-1}, M_w: 8200 g mol^{-1}, PDI: 1.03). For oligo(orcinol) synthesized by air as oxidant, low molar mass fraction formed 79% of the oligomer while (M_n: 1800 g mol^{-1}, M_w: 2400 g mol^{-1}, PDI: 1.33) higher one (M_n: 7600 g mol^{-1}, M_w: 7800 g mol^{-1}, PDI: 1.03) was found just 21% of it.

Figure 1 is FT-IR spectra for oligo(orcinol)s which were synthesized in different oxidants and for monomer. It is realized easily changes of after polymerization by looking over these spectrums. After polymerization, all peaks come out wide and shallow. It is because of increased molecule mass. That is to say, functional groups have different chemical surroundings, give near vibration signals and these causes to wide in FT-IR spectrum of oligomer. The bending vibration band of –OH group was observed at 1200 cm^{-1}. The bending vibration band of C–O–C was observed at 1170 cm^{-1}. This peak has showed to link of oxyphenylene. In FT-IR spectra, new peaks are seen around 1720 cm^{-1}. That is

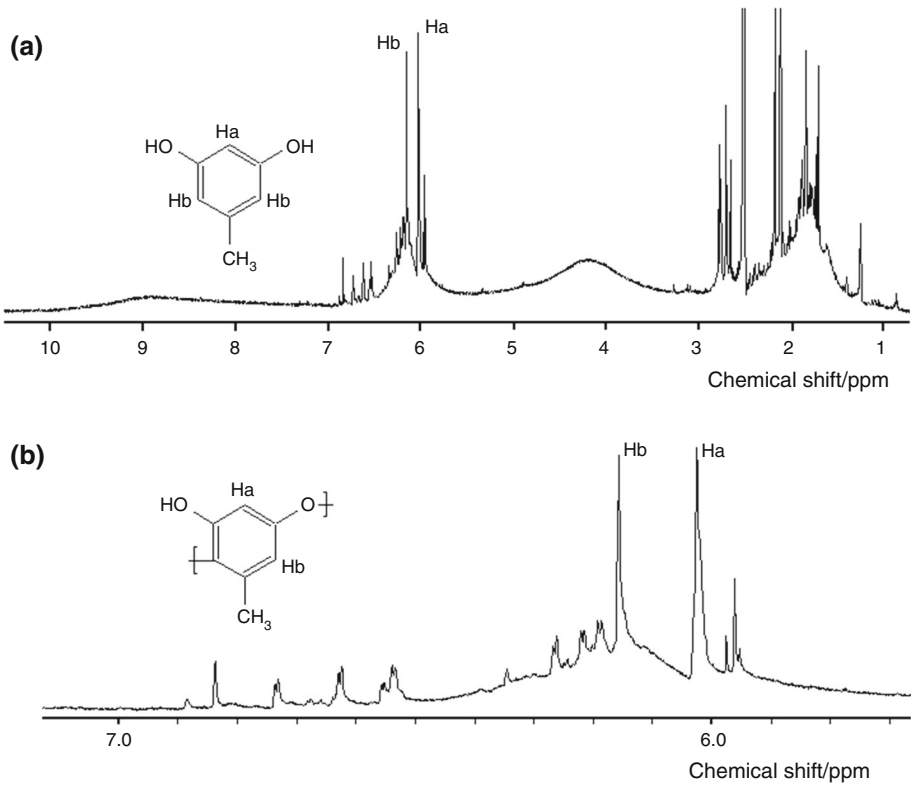

Fig. 2 ^{1}H-NMR spectra of orcinol monohydrate (**a**) and oligo(orcinol) (**b**)

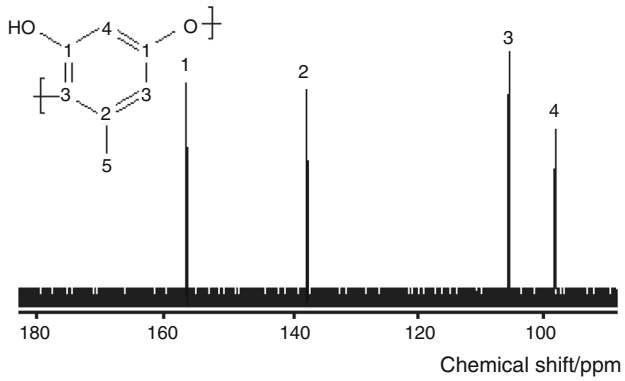

Fig. 3 ^{13}C-NMR spectrum of oligo(orcinol)

why protons of hydroxyl groups oxidize to quinone ones. Peaks at 1600 and 1450 cm^{-1} in spectrum belong to vibration of (C–C) bond. It points that new oligomer is formed neither phenylene nor oxyphenylene. At the end of oxidative polymerization of oligo(orcinol) with different oxidants is obtained black-colored product. This black colored product signalizes hydroxylation reaction, which is in the time of polymerization reaction, according to Hiroshi et al. [23, 24]. Other researchers [25, 26] reported resembling results. In the FT-IR spectra of monomer and oligomer, the region between 3000 to 3600 cm^{-1} shows –OH group and the hygroscopic water in oligomer. In the oligomer spectrum, vibration of –OH moves to high wavelengths; it is waited result.

Figure 2 shows ^{1}H-NMR spectra of orcinol monohydrate and oligo(orcinol) in d_6-DMSO. ^{1}H-NMR spectra of orcinol monohydrate had two singlet as 6.00 and 6.15 ppm. These singlet peaks in Fig. 2a correspond to H_a and H_b protons. Peak at 9.00 ppm is attributed to the proton of hydroxyl groups. The wide peak between 3 and 5 ppm is seen because of humidity in solvent. The signal of $–CH_3$ protons of monomer and oligomer was observed as singlet at 2.05 and 2.21 ppm, respectively. In the ^{1}H-NMR spectra of oligo(orcinol) (Fig. 2b), it is seen the peaks at 6.30 and 7.00 ppm are wide and shallow ones. The signals of H_a and H_b protons also shift to 6.18 and 6.26 ppm, respectively. These peaks belong to aromatic protons and in wide region looking at these protons show different kind of bonds (C–C and C–O–C) and this is responsive with NMR analysis.

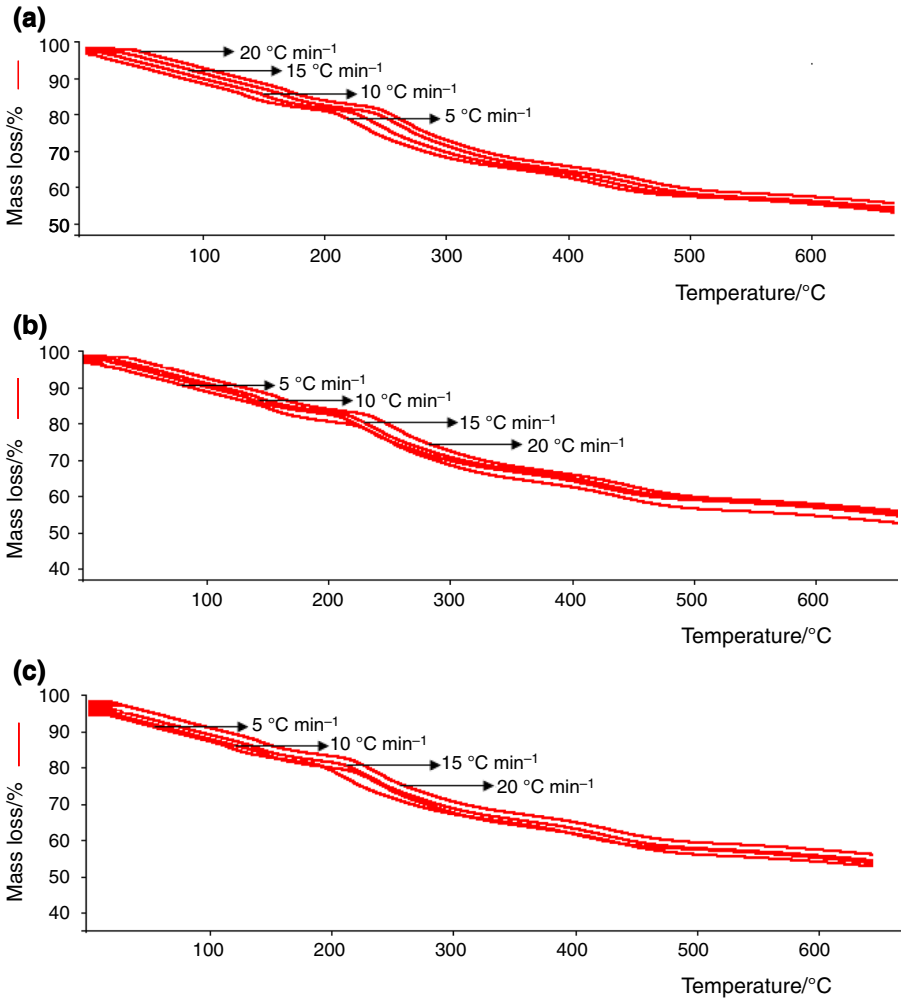

Fig. 4 The TG curves at different heating rates of oligo(orcinol)s, **a** NaOCl oxidant; **b** H_2O_2 oxidant; **c** air oxidant

Table 6 TG data for oligo(orcinol) obtained with different oxidants

Oligomer	Heating rate													
	5 °C min^{-1}				10 °C min^{-1}				15 °C min^{-1}				20 °C min^{-1}			
	T_i/°C	T_f/°C	T_{max}/°C	Mass loss/%	T_i/°C	T_f/°C	T_{max}/°C	Mass loss/%	T_i/°C	T_f/°C	T_{max}/°C	Mass loss/%	T_i/°C	T_f/°C	T_{max}/°C	Mass loss/%
Oligo(orcinol)[a]	76	570	300	57	78	578	323	56	80	581	338	53	81	583	350	53
Oligo(orcinol)[b]	74	582	237	55	78	585	254	55	81	576	264	54	83	579	270	53
Oligo(orcinol)[c]	73	563	236	56	75	568	250	52	76	573	301	53	77	573	305	54

T_i, initial degradation temperature/°C; T_f, final degradation temperature/°C; T_{max}, the temperature corresponding to maximum degradation rate/°C

[a]NaOCl oxidant

[b]H_2O_2 oxidant

[c]Air oxidant

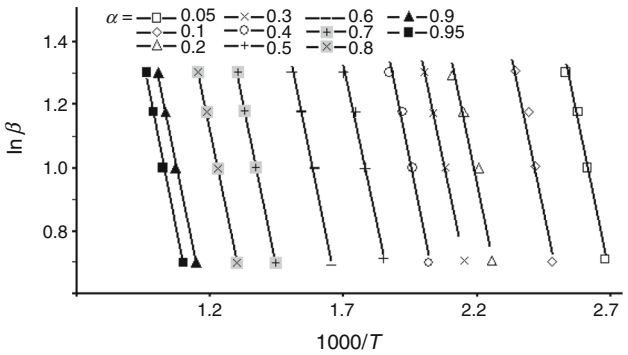

Fig. 5 FWO plots for the thermal degradation of oligo(orcinol) at varying conversion in N_2

The wide and shallow peaks between 8 and 10 ppm do not give spectra that belong to –OH proton signals. Nonetheless, it was seen that hydroxyl proton integration decreasing in comparison with aromatic protons. There can be two reasons: (i) due to hydrogen elimination end of type of oxyphenylene bond [27, 28] and (ii) phenolic groups change to quinone group during the polymerization with an effect of oxidant. Being nearly 5.9 ppm peaks built up quinolone formation. Also the signals between 1 to 2 ppm are shown aliphatic groups which have different chemical areas. Figure 3 shows ^{13}C-NMR spectrum of oligo(orcinol) in d_6-DMSO (between 100 to 210 ppm). The signals of methyl carbon atoms of monomer and oligomer were observed at 25 and 32 ppm, respectively. Near four main carbon signals, with so many small emphases aromatic carbon signals show that different connected aromatic carbon signals and this is compatible with results of ^{13}C-NMR analysis.

Thermal stability

The non-isothermal TG curves of the oligo(orcinol)s were recorded, at heating rates of 5, 10, 15, 20 °C min^{-1} under a nitrogen flow with a flow rate of 200 mL min^{-1}. The TG curves at different heating rates of oligo(orcinol)s synthesized by NaOCl, H_2O_2 and air as oxidant are given in Fig. 4. Initial and final temperatures of the curves, the temperatures corresponding to maximum degradation rate and percent mass loss were determined from TG curves. Also, it was shown that with increase in the mole mass of the polymers the initial temperature of the degradation and stabilization increased. In the end of this degradation, obtained carbon residue also increased with increasing heating rate. This is exactly about structure of oligo(orcinol); in other words it is about percent of oxyphenylene-phenylene. Thermal data that were obtained from TG curves of oligo(orcinol) with different molar mass are shown in Table 6. In Table 6 it is shown that the thermal

Table 7 Activation energy and regression coefficient values calculated by Tang, KAS, and FWO methods for oligo(orcinol) synthesized with NaOCl oxidant

Degradation fraction	E_{Tang}/kJ mol^{-1}	R^2	E_{KAS}/kJ mol^{-1}	R^2	E_{FWO}/kJ mol^{-1}	R^2
0.05	71.33	0.9813	79.23	0.9815	68.98	0.9813
0.1	72.49	0.9981	72.16	0.9887	83.74	0.9890
0.2	87.13	0.9961	86.71	0.9854	88.83	0.9954
0.3	86.13	0.9832	85.71	0.9886	89.20	0.9911
0.4	86.54	0.9714	86.13	0.9851	89.20	0.9717
0.5	88.71	0.9811	88.21	0.9916	89.20	0.9935
0.6	85.71	0.9967	85.30	0.9935	89.20	0.9937
0.7	85.13	0.9823	84.55	0.9952	89.20	0.9951
0.8	80.23	0.9845	79.73	0.9913	85.56	0.9847
0.9	72.08	0.9923	71.50	0.9952	78.27	0.9890
0.95	50.71	0.9847	49.96	0.9968	58.25	0.9914
Mean	78.74		79.02		81.78	

Table 8 Activation energy and regression coefficient values calculated by Tang, KAS, and FWO methods for oligo(orcinol) synthesized with H_2O_2 oxidant

Degradation fraction	E_{Tang}/kJ mol^{-1}	R^2	E_{KAS}/kJ mol^{-1}	R^2	E_{FWO}/kJ mol^{-1}	R^2
0.05	30.00	0.9432	31.04	0.9565	30.11	0.9689
0.1	56.95	0.9821	44.23	0.9812	49.15	0.9651
0.2	75.24	0.9678	74.82	0.9711	78.09	0.9879
0.3	75.40	0.9942	74.82	0.9965	79.00	0.9657
0.4	73.16	0.9890	73.74	0.9523	77.36	0.9980
0.5	68.34	0.9845	72.74	0.9890	76.82	0.9765
0.6	69.58	0.9898	69.00	0.9921	76.45	0.9980
0.7	67.17	0.9643	66.42	0.9987	75.73	0.9851
0.8	64.68	0.9811	63.93	0.9112	74.82	0.9811
0.9	67.17	0.9971	65.68	0.9871	77.55	0.9851
0.95	115.8	0.9641	115.3	0.9768	125.0	0.9656
Mean	69.42		66.88		73.65	

Table 9 Activation energy and regression coefficient values calculated by Tang, KAS, and FWO methods for oligo(orcinol) synthesized with air oxidant

Degradation fraction	E_{Tang}/kJ mol^{-1}	R^2	E_{KAS}/kJ mol^{-1}	R^2	E_{FWO}/kJ mol^{-1}	R^2
0.05	22.44	0.9823	22.61	0.9845	27.12	0.9838
0.1	34.08	0.9854	33.25	0.9962	38.59	0.9983
0.2	34.41	0.9978	33.25	0.9868	38.59	0.9990
0.3	34.25	0.9926	33.25	0.9915	39.32	0.9842
0.4	34.17	0.9990	33.25	0.9771	39.86	0.9818
0.5	32.25	0.9826	34.08	0.9889	40.41	0.9928
0.6	29.93	0.9961	30.76	0.9826	39.32	0.9981
0.7	31.51	0.9962	30.64	0.9880	38.95	0.9839
0.8	31.65	0.9860	30.63	0.9838	38.41	0.9942
0.9	39.90	0.9912	39.07	0.9978	51.88	0.9890
0.95	48.22	0.9941	47.38	0.9811	60.62	0.9817
Mean	33.89		33.46		41.19	

stability in oligo(orcinol) is proportional to an increase with the molecular mass distribution or at the heating rate. Generally, this increasing takes place from lower molecular mass distribution to higher one or from lower heating rate to higher one.

Determination of kinetic parameters related to the solid-state degradation of oligo(orcinol)

Thermal degradation kinetics of all the oligo(orcinol) was investigated by TG technique. All the TG curves of

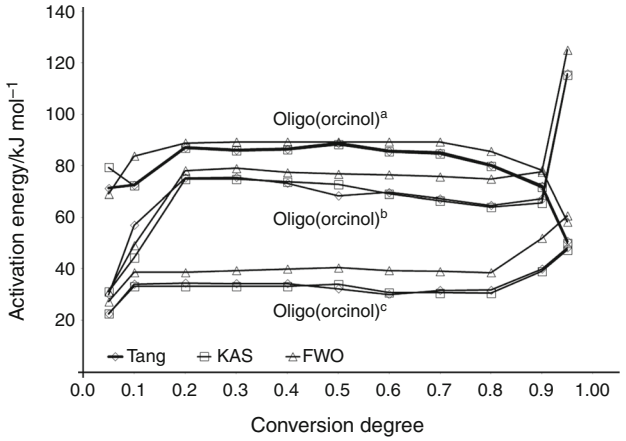

Fig. 6 The activation energy values versus degree of conversion for oligo(orcinol)s, **a** NaOCl oxidant; **b** H_2O_2 oxidant; **c** air oxidant

oligo(orcinol)s with different molar mass exhibit a single degradation stage. The kinetic analysis of the thermogravimetric data of oligo(orcinol) was studied by using the model-free methods. FWO, KAS and Tang as model-free methods were used in this study. Accordingly the kinetic parameters were determined by non-isothermal methods. Variation of the kinetic parameters related to the degradation with the molar mass was also investigated. TG technique was used to investigate thermal degradation kinetics of oligomer. The first thermogravimetric method used to calculate the kinetic parameters of oligomer in this work is those of Tang. The Tang method which is not dependent on the reaction mechanism was used to calculate the kinetic parameters of the thermal degradation of polymers with different molar masses. The average activation energy values related to thermal degradation of oligo(orcinol) synthesized with NaOCl, H_2O_2 and air oxidants were found to be 78.74, 69.42, and 33.89 kJ mol^{-1}, respectively. The other methods used for calculating kinetic parameters of oligo(orcinol) were those of Flynn–Wall–Ozawa and Kissinger–Akahira–Sunose. The Flynn–Wall–Ozawa method is an integral method, and the so-called Eq. (4) suggested by FWO can be used in logarithmic form for determining the activation energy of a solid-state thermal degradation process. Figure 5 illustrates the plots of ln β versus 1000/T of the thermal degradation stage of oligo(orcinol) at varying conversions. Constant mass loss lines were determined by measuring the temperature at a given mass percent for each rate. According to FWO method, the average activation energy values of oligo(orcinol) synthesized with NaOCl, H_2O_2 and air oxidants were found as 81.78, 73.65 and 41.19 kJ mol^{-1}, respectively. Equation (2) suggested by KAS was also utilized to determine the values of activation energy from plots of $\ln(\beta/T^2)$ against $1/T$ over a wide range of conversion. The results obtained by KAS method were found as 79.02, 66.88 and 33.46 kJ mol^{-1}, respectively, for oligo(orcinol) synthesized with NaOCl, H_2O_2 and air oxidants and α was over the range of $0.05 < \alpha < 0.95$. Consequently, the activation energies (E) values calculated from all mathematical methods for thermal degradation stages of oligo(orcinol) were very close to each other. The activation energy (E) values and regression coefficients (R^2) obtained by the FWO, Tang and KAS methods for all the thermal degradation of oligo(orcinol) are summarized in Tables 7, 8 and 9. The acceptable correlation coefficient-r values found for each conversion degree are always reasonably high.

The results obtained by using several methods based on multiple heating rates show that activation energy increased with an increase in molar mass. Figure 6 shows the activation energy values versus degradation fraction for all polymers. The activation energy values for 5% mass loss of oligo(orcinol) synthesized with NaOCl, H_2O_2 and air oxidants were calculated as 68.98, 30.00, and 22.44 kJ mol^{-1}, respectively. The activation energy values of oligo(orcinol) synthesized with NaOCl, H_2O_2, and air oxidants were calculated as 49.96, 115.3 and 48.22 kJ mol^{-1} for 95% mass loss.

When Fig. 6 is examined carefully, it can be seen that the activation energy values are constant in the range of 0.1–0.9 of conversion degree for oligo(orcinol) synthesized with NaOCl and air oxidants and in the range of 0.2–0.9 of conversion degree for oligo(orcinol) synthesized with H_2O_2 oxidants. Therefore, degradation process for all of the so-called oligomer is not depending on conversion degree in this range. The results obtained by using all the methods also show that activation energy increased with an increase in molar mass.

Conclusions

The oxidative polymerization of oligo(orcinol) was studied by air, H_2O_2 and NaOCl as an oxidant in alkaline medium between 40 and 90 °C. The structure of synthesized oligo(orcinol) was confirmed by FT-IR, ^{1}H-NMR and ^{13}C-NMR. The characterization of oligo(orcinol) was determined with TG, size exclusion chromatography (SEC), and solubility tests. Experimental results exhibited NaOCl oxidant was a more effective oxidant in the conversion to oligomer of orcinol. The optimum reaction condition for NaOCl oxidant was found to be $[orcinol]_0$ = 0.0144 mol L^{-1}, $[KOH]_0$ = 0.024 mol L^{-1} and $[NaOCl]_0$ = 0.04 mol L^{-1}, at 70 °C for 10 h. The % conversion values to oligomer of orcinol were determined as 21, 42, and 62% for air, H_2O_2, and NaOCl oxidants, respectively, under optimum reaction conditions. According to SEC analysis, values of M_n and PDI of oligo(orcinol)

were found to be 2170 g mol^{-1} and 1.14; 1500 g mol^{-1} and 1.18; 2260 g mol^{-1} and 1.12 for H_2O_2, air, and NaOCl oxidants, respectively. As a result of kinetic studies, by FWO, Tang and KAS as multiple heating rate methods, it was investigated the molar mass affection on kinetic parameters. According to obtained results, it was seen that by increasing molar mass the activation energy increased, too.

References

1. Doğan F, Kaya İ, Temizkan K. Template-free oxidative synthesis of polyaminonaphthol nanowires. Eur Polym J. 2015;66:397–406.
2. Hammerschmidt S, Wahn H. The oxidants hypochlorite and hydrogen peroxide induce distinct patterns of acute lung injury. Biochim Biophys Acta (BBA) Mol Basis Dis. 2004;1690:258–64.
3. Kobayashi S, Higashimura H. Oxidative polymerization of phenols revisited. Prog Polym Sci. 2003;28:1015–48.
4. Hay AS, Blanchard HS, Endres GF, Eustance JW. Polymerization by oxidative coupling. J Am Chem Soc. 1959;81:6335–6.
5. Doğan F, Kaya İ, Temizkan K. Multi-response behavior of aminosulfonaphthole system. J Mol Catal B Enzym. 2016;133:234–45.
6. Doğan F, Kaya İ, Temizkan K. Regioselectively functionalized synthesis of poly(amino naphthalene disulfonic acid). Synth Met. 2016;215:77–85.
7. Doğan F, Kaya İ, Temizkan K. A novel shape-controlled synthesis of bifunctional organic polymeric nanoparticles. Polymer. 2015;70:59–67.
8. Doğan F, Kaya İ, Temizkan K. Synthesis route to regioselectively functionalized bifunctional polyarene. Polym Int. 2015;64:1639–48.
9. Chauhan NPS. Thermal curing and degradation kinetics of terpolymer resins derived from vanillin oxime, formaldehyde and *p*-chloro-/*p*-methylacetophenone. Korean J Chem Eng. 2015;32(3):552–62.
10. Chauhan NPS, Mozafari M, Ameta R, Punjabi PB, Ameta SC. Spectral and thermal characterization of halogen-bonded novel crystalline oligo(p-bromoacetophenone formaldehyde). J Phys Chem B. 2015;119(7):3223–30.
11. Chauhan NPS. Spectral and thermal investigation of designed terpolymers bearing p-acetylpyridine oxime moieties having excellent antimicrobial properties. Des Monomers Polym. 2013;16(6):543–55.
12. Tang W, Liu Y, Zhang CH, Wang C. New approximate formula for Arrhenius temperature integral. Thermochim Acta. 2003;408:39–43.
13. Kissinger E. Reaction kinetics in different thermal analysis. Anal Chem. 1957;29:1702–5.
14. Akahira T, Sunose T. Method of determining activation deterioration constant of electrical insulating materials. Res Rep Chiba Inst Technol (Sci Technol). 1971;16:22–31.
15. Chauhan NPS. Isoconversional curing and degradation kinetics study of self-assembled thermo-responsive resin system bearing oxime and iminium groups. J Macromol Sci Part A. 2012;49(9):706–19.
16. Chauhan NPS. Terpolymerization of *p*-acetylpyridine oxime, *p*-methylacetophenone and formaldehyde, and its thermal studies. J Therm Anal Calorim. 2012;110(3):1377–88.
17. Flynn JH, Wall LA. General treatment of the thermogravimetry of polymers. J Res Nat Bur Stand Part A. 1966;70:487–523.
18. Ozawa T. A new method of analysing thermogravimetric data. Bull Chem Soc Jpn. 1965;38:881–2.
19. Chauhan NPS. Facile synthesis of environmental friendly halogen-free microporous terpolymer from renewable source with enhanced physical properties. Des Monomers Polym. 2012;15(6):587–600.
20. Doğan F, Temizkan K, Kaya İ. Regioselective synthesis of polygamma (γ) acid. RSC Adv. 2015;5:53369–80.
21. Baran NY, Saçak M. Synthesis, characterization and molecular weight monitoring of a novel Schiff base polymer containing phenol group: thermal stability, conductivity and antimicrobial properties. J Mol Struct. 2017;1146:104–12.
22. Kaya İ, Doğan F, Bilici A. Schiff base-substituted polyphenol: synthesis, characterisation and non-isothermal degradation kinetics. Polym Int. 2009;58:570–8.
23. Kadota J, Fukuoka T, Uyama H, Hasegawa K, Kobayashi S. New positive-type photoresists based on enzymatically synthesized polyphenols. Macromol Rapid Commun. 2004;25:441–4.
24. Kurisawa M, Chung JE, Uyama H, Kobayashi S. Laccase catalyzed synthesis and antioxidant property of poly (catechin). Macromol Biosci. 2003;3:758–64.
25. Doğan F, Bilici A, Yıldırım M, Kaya İ. 6-Hydroxyquinoline oligomers emit white light. Sci Adv Mater. 2014;6:1957–64.
26. Bilici A, Doğan F, Yıldırım M, Kaya İ. Facile and regioselective synthesis of poly(5-hydroxyquinoline). React Funct Polym. 2011;71:675–83.
27. Uyama H, Maruichi N, Tonami H, Kobayashi S. Peroxidase-catalyzed oxidative polymerization of bisphenols. Biomacromol. 2002;3:187–93.
28. Kobayashi S, Uyama H, Kimura S. Enzymatic polymerization. Chem Rev. 2001;101:3793–818.